Jpn. J. Appl. Phys. Vol. 41 (2002) pp. 227–231
Part 1, No. 1, January 2002

Influences of Point and Extended Defects on As Diffusion in Si

Ryangsu KIM*, Tetsuya HIROSE, Toshihumi SHANO, Hiroshi TSUJI and Kenji TANIGUCHI

Department of Electronics and Information Systems, Osaka University, Osaka 565-0871, Japan

(Received July 31, 2001; accepted for publication September 17, 2001)

The influences of point and extended defects introduced by ion implantation on the transient enhanced diffusion (TED) of As have been examined. The implantation of a subamorphizing dose of Si into Si wafers with nearly uniform As background doping results in the slight segregation of As into {311} defects after annealing at 670°C, whereas an amorphizing dose of Si is found to induce significant segregation of As into end-of-range (EOR) dislocation loops after annealing at 820°C, regardless of the background As concentration. In the second experiment, As ions were implanted into Si wafers at 30 keV to low and medium doses. Some of the wafers were preannealed in order to recrystallize the amorphous layer and subsequently implanted with subamorphizing doses of Si at 50 keV. The resulting profiles reveal that the TED of As increases with Si implantation dose, indicating that transient As diffusion occurs via Si self-interstitials in the same way as for B and P. A suppression of the TED of As in the early stages of annealing at higher As and Si implantation doses is also observed. This is considered to originate from the formation of immobile arsenic-vacancy clusters. [DOI: 10.1143/JJAP.41.227]

KEYWORDS: arsenic, interstitial, vacancy, {311} defect, end-of-range dislocation loop

1. Introduction

Arsenic is widely used as an n-type dopant in the fabrication of silicon integrated circuits. Arsenic atoms implanted into Si wafers exhibit transient enhanced diffusion (TED) during subsequent annealing.[1)] Extensive studies have clarified[1–5)] that the presence of excess Si self-interstitials in the Si wafer is responsible for the TED of B and P, and allows TED to occur simultaneously with the release of self-interstitials trapped in the {311} defects.

When the implantation dose of As exceeds the amorphizing threshold ($\sim 1 \times 10^{13}\,\mathrm{cm}^{-2}$), the implanted region becomes amorphous,[6,7)] leaving excess self-interstitials in a region beyond the amorphous/crystalline interface called the end-of-range (EOR) region. During postimplantation annealing, the interstitials accumulate to form EOR defects, while the amorphous layer recrystallizes epitaxially in the solid phase. The majority of EOR defects after short periods of annealing are {311} defects, which become the source of self-interstitials for the formation of {111} and {100} dislocation loops upon further annealing.[8)] The interstitials which escape from absorption by dislocation loops and recombination with vacancies or at the surface, are expected to allow the TED of As.

It has been reported that B atoms preferentially segregate into {311} defects,[9)] and that B[10)] and P[11,12)] segregate into EOR dislocation loops. However, although there has been a report[13)] that an increase in the background As concentration reduces the amount of interstitials trapped in {311} defects, little attention has been paid to the segregation of As into EOR defects. It is thought that such segregation may affect the TED of As.

Recently, new doping approaches[14,15)] involving subamorphizing Si implantation prior to dopant implantation have been examined in order to minimize the channeling and TED of B, P and As to achieve shallower junctions compared to single dopant implantation. The optimization of subamorphizing Si preimplantation will allow excess vacancies to be created in the region that is to be subsequently implanted with dopants. This technique also inserts excess interstitials into the area beyond the excess vacancy region, resulting in an anticipated increase in the TED of dopants during postimplantation annealing. These features make this technique useful for examining the interaction of As with excess vacancies and excess interstitials.

In this paper we clarify the interaction of As atoms with {311} defects and dislocation loops formed by Si self-implantation and examine the effects of excess vacancies and interstitials introduced by subamorphizing Si implantation on the diffusion of implanted As.

2. Experimental Procedures

Figure 1(a) shows the procedure of the first experiment. The segregation of As into extended defects was examined using (100) Czochralski Si wafers with nearly uniform As background doping at 2.0×0^{17} to $5.5 \times 10^{19}\,\mathrm{cm}^{-3}$. The arsenic doping was performed by implanting As at 100 keV to various doses followed by annealing at 1100°C for 5 h. {311} defects were formed by Si ion implantation at 50 keV to a subamorphizing dose of $1 \times 10^{14}\,\mathrm{cm}^{-2}$ followed by postimplantation annealing at 670°C for 30 and 330 min. EOR dislocation loops were generated by implanting Si ions at 50 keV to an amorphizing dose of $5 \times 10^{15}\,\mathrm{cm}^{-2}$ followed by annealing at 820°C for 20 s and 10 min. The flow chart in Fig. 1(b) shows the procedure of the second experiment. As ions were also implanted into p-type (100) Czochralski Si wafers at 30 keV to amorphizing doses of 5×10^{13} to $5 \times 10^{15}\,\mathrm{cm}^{-2}$, followed by postimplantation annealing at 720°C for 30 min.

The effect of excess vacancies and interstitials was examined using the p-type Si wafers described above implanted with As ions at 30 keV to amorphizing doses of 5×10^{13} and $5 \times 10^{14}\,\mathrm{cm}^{-2}$, as shown in Fig. 1(c). After implantation, one group of wafers was processed as follows. The wafers were preannealed at 550°C for 10 min in order to recrystallize the amorphous layer formed by As implantation, followed by Si ion implantation at 50 keV to subamorphizing doses of 1×10^{13}, 5×10^{13}, and $1 \times 10^{14}\,\mathrm{cm}^{-2}$ or 15 keV to a dose of $5 \times 10^{13}\,\mathrm{cm}^{-2}$. All wafers were finally annealed at 820°C for 1–300 min.

All annealing was performed in N_2 ambient in a preheated vertical furnace tube in order to minimize ramp-up and

*E-mail: kim@eie.eng.osaka-u.ac.jp

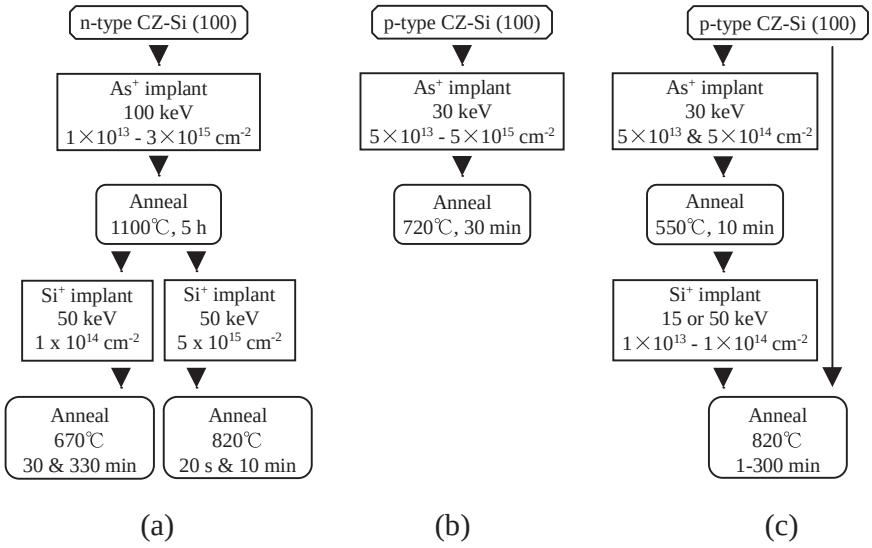

Fig. 1. Flow charts of experimental procedures.

ramp-down times. The resulting dopant profiles were analyzed by secondary ion mass spectroscopy (SIMS) using a Physical Electronics 6600 mass spectrometer.

3. Results

3.1 Segregation of As into extended defects

Figure 2 shows the As profiles of samples subjected to subamorphizing Si implantation at 50 keV to a dose of $1 \times 10^{14}\,\mathrm{cm}^{-2}$ and subsequently annealed at 670°C for 30 and 330 min. Judging from the segregation of B into {311} defects,[9] the thickness of the {311} defect layer ranges from approximately 40 to 160 nm. Slight segregation of As in the defect layer was observed after annealing for 330 min, which produces {311} defects visible by plan-view transmission electron microscopy (PTEM).[16] The segregation kinetics appears similar to that of B,[9] that is, the number of impurities segregated into {311} defects increases with annealing time up to the onset of defect dissolution.

The SIMS profiles for the As-doped samples implanted with Si at 50 keV to an amorphizing dose of $5 \times 10^{15}\,\mathrm{cm}^{-2}$ and then annealed at 820°C are shown in Fig. 3. It is evident that segregation of As occurs in all of the samples to a much greater extent than the segregation into {311} defects shown in Fig. 2. The segregation peak position in each sample is almost the same, and coincides with the layer of EOR dislocation loops, as determined from the cross-sectional TEM analysis.[17] These results also indicate that the segregation of As is nearly independent of the background As concentration, and the amount of segregated As increases with annealing time. Since annealing at 820°C for 20 s is insufficient for all of the excess interstitials to be accumulated into EOR dislocation loops, the degree of segregation in Fig. 3 is much lower than that after annealing for 10 min at the same temperature.

The estimated areal densities of As segregated into EOR dislocation loops after annealing for 10 min, based on a Gaussian fit, are listed in Table I for the three samples doped with different As backgrounds in Fig. 3. The areal density of

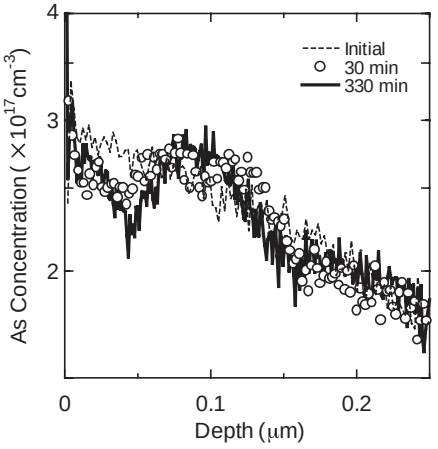

Fig. 2. SIMS profiles of As for As-doped samples implanted with Si at 50 keV to a subamorphizing dose of $1 \times 10^{14}\,\mathrm{cm}^{-2}$ followed by annealing at 670°C for 30 min (solid curve) and 330 min (open circles). Broken curve represents initial profile of As.

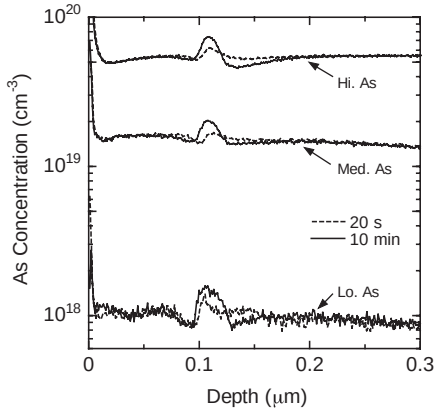

Fig. 3. SIMS profiles of As for As-doped samples implanted with Si at 50 keV to an amorphizing dose of $5 \times 10^{15}\,\mathrm{cm}^{-2}$ followed by annealing at 820°C for 20 s (broken curves) and 10 min (solid curves). Background As levels of each sample are $1.0 \times 10^{18}\,\mathrm{cm}^{-3}$ (Lo. As), $1.5 \times 10^{19}\,\mathrm{cm}^{-3}$ (Med. As), and $5.5 \times 10^{19}\,\mathrm{cm}^{-3}$ (Hi. As).

Table I. Difference in segregation energy toward EOR dislocation loops between As and B, extracted from samples with various As background concentrations. Last column lists segregation energies of As when that of B is 0.75 eV.[10)]

Sample	Q^{As} (cm^{-2})	C_f^{As} (cm^{-3})	$E_{seg}^{As} - E_{seg}^{B}$ (eV)	E_{seg}^{As} (eV)
Low As	1.50×10^{12}	8.76×10^{17}	−0.11	0.64
Med As	1.05×10^{13}	1.43×10^{19}	−0.19	0.56
Hi As	4.00×10^{13}	4.90×10^{19}	−0.18	0.57

impurity atoms segregated into EOR dislocation loops at equilibrium has been given as[10)]

$$Q = A\bar{r}DC_f \exp\left(\frac{E_{seg}}{k_B T}\right), \tag{3.1}$$

where A is a constant, $\bar{r}$ and D are the average radius and areal density of EOR dislocation loops, respectively, C_f is the impurity concentration in Si (around EOR dislocation loops) and E_{seg} is the segregation energy of impurities. PTEM analysis is indispensable for measuring $\bar{r}$ and D; however, it is possible to determine the segregation energy of As (E_{seg}^{As}) without knowing $\bar{r}$ and D. The areal density of B segregated into EOR dislocation loops is known[18)] to be $3.07 \times 10^{12}\,cm^{-2}$ in uniformly B-doped samples (9.2×10^{17} cm^{-3}) preimplanted and annealed under the same conditions as in the present experiment (Si at 50 keV and $5\times 10^{15}\,cm^{-2}$; annealing at 820°C for 10 min). Therefore, assuming that neither background dopant species nor background As levels of up to $5.5 \times 10^{19}\,cm^{-3}$ (highest level in present experiment) affect $\bar{r}$ and D, E_{seg}^{As} is given, according to eq. (3.1), by

$$E_{seg}^{As} = E_{seg}^{B} + k_B T \ln\left(\frac{Q_{As}C_f^{B}}{Q_B C_f^{As}}\right), \tag{3.2}$$

where the superscripts *As* and *B* of E_{seg}, Q, and C_f denote the values for As and B, respectively. Table I lists the calculated differences between the segregation energies of As and B in each sample, as estimated from eq. (3.2). The dispersion of these energy differences is relatively small regardless of the background As level. Consequently, it is considered that neither the concentration of As nor the density of electrons affects $\bar{r}$ and D. Assuming the segregation energy of B is 0.75 eV,[10)] the segregation energy of As in each sample will be as shown in Table I. We found that the segregation energy of As, approximately 0.6 eV, is lower than the reported value (0.9 eV) based on *ab initio* calculations.[19)] The lower segregation energy is thought to originate from the fact that the segregation energy derived from our experiments is averaged over all of the energies of possible segregation for all EOR dislocation loop radii. This hypothesis will need to be verified by *ab initio* calculations.

We performed an experiment in order to verify the segregation of As into EOR defects for single As implantation. Arsenic ions with various doses were implanted into p-type Si wafers. Figure 4 shows the As profiles for samples implanted with As at 30 keV to doses of 5×10^{13} to $5 \times 10^{15}\,cm^{-2}$ and subsequently annealed at 720°C for 30 min. Postimplantation profiles of As are also shown for doses of 5×10^{13}, 5×10^{14}, and $5 \times 10^{15}\,cm^{-2}$. As expected from the experimental results in Fig. 3, the segregation of As into EOR defects occurs in the 40–60 nm region in all

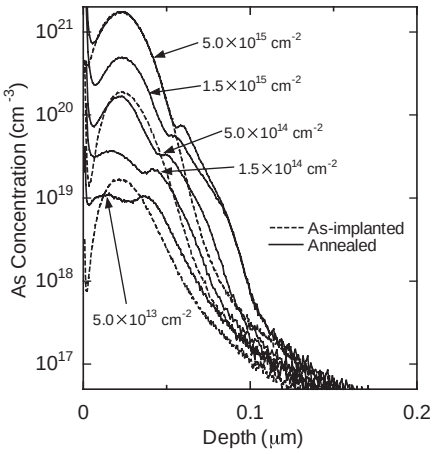

Fig. 4. SIMS profiles of As for samples implanted with As at 30 keV to doses ranging from 5×10^{13} to $5 \times 10^{15}\,cm^{-2}$ followed by annealing at 720°C for 30 min (solid curves). Postimplantation profiles of As are also shown for samples implanted with Si to doses of 5×10^{13}, 5×10^{14}, and $5 \times 10^{15}\,cm^{-2}$ (broken curves).

samples. The shift of the segregation peak to deeper regions arises from the increase in thickness of the amorphous layer which is a function of the As implantation dose.[7)] Hence, the segregation in Fig. 4 is attributed to the existence of EOR dislocation loops and {311} defects, with segregation into EOR dislocation loops being dominant. The results of our experiments indicate that the kink in the As profile in the early stage of annealing at 720°C for 30 min is due to the segregation of As into EOR defects.

3.2 *Transient enhanced diffusion of As due to subamorphizing postimplantation of Si*

Experiments on Si postimplantation enable us to directly compare the net enhancement of As diffusion in samples with and without Si implantation, whereas Si preimplantation reduces As channeling,[15)] making direct comparison impossible. SIMS profiles of As for samples implanted with As or As and Si to a subamorphizing dose of $5 \times 10^{13}\,cm^{-2}$ at 50 keV after annealing at 820°C are shown in Figs. 5 and

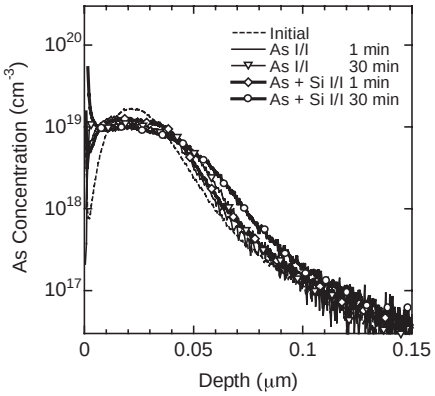

Fig. 5. SIMS profiles of As for samples implanted with As at 30 keV to a dose of $5 \times 10^{13}\,cm^{-2}$ with (thick curves) and without (thin curves) subamorphizing Si implantation at 50 keV to a dose of $5 \times 10^{13}\,cm^{-2}$, and subsequently annealed at 820°C for 1 and 30 min. Si-implanted samples were preannealed at 550°C for 10 min in order to recrystallize the amorphous layer created by As implantation.

6 for As doses of 5×10^{13} and $5 \times 10^{14}\,cm^{-2}$, respectively. The two figures show the extra TED of As for As and Si implantation after annealing for 30 min compared to that for single As implantation. This demonstrates that the TED of As occurs primarily via self-interstitials, as evidenced by the enhancement of TED due to the excess interstitials generated by the additional Si implantation.

It can also be seen in Fig. 6 that the additional Si implantation slightly suppresses the TED of As during the first minute of annealing at 820°C. This initial suppression is not observed in Fig. 5 for the samples implanted with a lower dose of As ($5 \times 10^{13}\,cm^{-2}$). Figure 7 shows the movement of the As tail at $2 \times 10^{18}\,cm^{-3}$ from the SIMS profiles of samples implanted with As to a dose of $5\times 10^{14}\,cm^{-2}$ and with Si to doses of between 1×10^{13} and $1 \times 10^{14}\,cm^{-2}$, followed by annealing at 820°C for 1 to 300 min. The initial suppression and the additional TED during subsequent annealing occur when the Si dose exceeds $5 \times 10^{13}\,cm^{-2}$. This initial suppression and subsequent increase in the TED of As are considered to be a result of the effect of large amounts of Si implantation damage at As concentrations exceeding $1 \times 10^{19}\,cm^{-3}$.

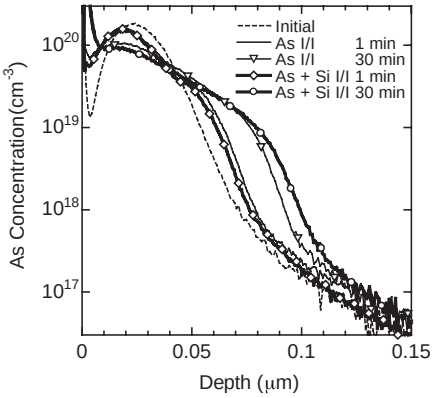

Fig. 6. SIMS profiles of As for samples implanted with As at 30 keV to a dose of $5 \times 10^{14}\,cm^{-2}$ with (thick curves) and without (thin curves) subamorphizing Si implantation at 50 keV to a dose of $5 \times 10^{13}\,cm^{-2}$, and subsequently annealed at 820°C for 1 and 30 min. Si-implanted samples were preannealed at 550°C for 10 min in order to recrystallize the amorphous layer created by As implantation.

It is conceivable that the formation of arsenic–vacancy (As–V) clusters is responsible for the initial suppression. There have been many studies on examining As clusters of two to four As atoms and one vacancy,[20–22] as generated when As concentrations exceed the solid solubility limit. In our experiment (Fig. 6), the projected range (R_p) of Si implanted at 50 keV is approximately 73 nm, and excess vacancies lie between the surface and a depth of approximately $0.8R_p$[23] (~58 nm). The excess vacancy region overlaps the distribution of implanted As in Fig. 6, except for the channeling tail of As. Consequently, in the initial stage of postimplantation annealing, As–V clustering may occur due to the presence of excess vacancies and the high As concentration around the peak of the As profile. These clusters directly prevent As from diffusing from the R_p of As to deeper regions.

The effect of excess vacancies on the TED of As was further examined by implanting Si ions to a dose of $5\times 10^{13}\,cm^{-2}$ at 15 keV ($R_p \sim 24$ nm) into the wafer previously implanted with As to $5 \times 10^{14}\,cm^{-2}$. This Si implantation has the same dose but a lower energy than that for the previous experiment (Fig. 6). The lower Si implantation energy was chosen in order to distribute the excess vacancies between the surface and a depth of ~18 nm and excess interstitials in the R_p of As and deeper regions. Figure 8 shows a comparison of As profiles for the samples implanted with As and the samples implanted with As and Si at 15 keV after annealing at 820°C. It can be seen that after annealing for 1 min there is little difference in the As tails between the Si-implanted and non-Si-implanted samples. This supports the conclusion that the initial suppression of the TED of As as a result of 50 keV Si implantation (Fig. 6) arises from As–V clustering induced by the overlap of the excess vacancy regions with the implanted As. Figure 8 shows that As diffusion is enhanced slightly with annealing for a further 30 min due to the presence of excess interstitials from the additional Si implantation compared to the case of single As

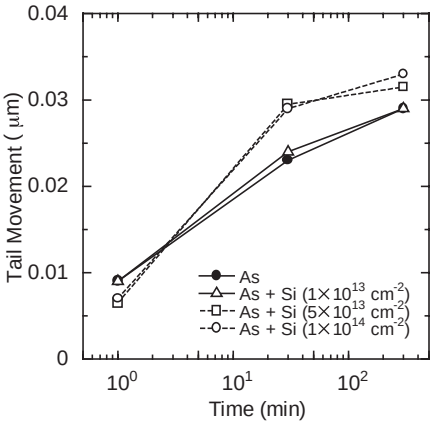

Fig. 7. Movement of As tails from SIMS profiles at $2 \times 10^{18}\,cm^{-3}$ for samples implanted with As at 30 keV to a dose of $5 \times 10^{14}\,cm^{-2}$ with (closed circles) and without (open symbols) subamorphizing Si implantation at 50 keV, and subsequently annealed at 820°C for 1, 30 and 300 min. Si doses are 1×10^{13}, 5×10^{13}, and $1 \times 10^{14}\,cm^{-2}$.

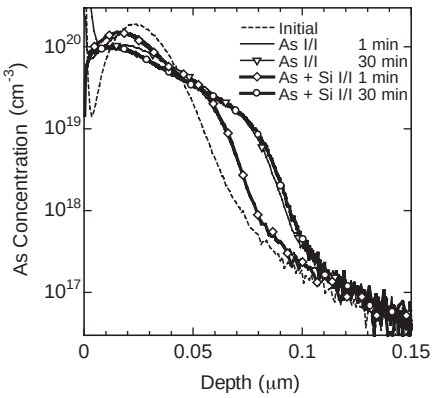

Fig. 8. SIMS profiles of As for samples implanted with As at 30 keV to a dose of $5 \times 10^{14}\,cm^{-2}$ with (thick curves) and without (thin curves) subamorphizing Si implantation at 15 keV to a dose of $5 \times 10^{13}\,cm^{-2}$, and subsequently annealed at 820°C for 1 and 30 min. Si-implanted samples were preannealed at 550°C for 10 min in order to recrystallize the amorphous layer created by As implantation.

implantation.

In addition to As–V clustering, vacancy clustering[24,25] is expected to contribute to the initial suppression of the TED of As. Vacancy clusters are available to recombine with the excess interstitials, further inhibiting transient As diffusion via interstitials. Although vacancy clusters are thought to be introduced by the additional Si implantation at lower As doses of $5 \times 10^{13}\,\mathrm{cm}^{-2}$, no initial suppression is observed in Fig. 5. The recombination of vacancy clusters with excess interstitials therefore contributes much less to the suppression of transient As diffusion than As–V clustering.

4. Conclusion

The influence of extended defects on the TED of As has been investigated by implanting Si into Si wafers with nearly uniform As background doping. We found that As atoms segregate into {311} defects much less than into EOR dislocation loops, and from the areal density of As segregated into EOR dislocation loops, the segregation energy of As into the defects was calculated to be approximately 0.6 eV, which is smaller than that of B.

Experimental results for subamorphizing Si implantation at 50 keV after As implantation reveal that the TED of As increases with the Si implantation dose, demonstrating that the TED of As occurs primarily via Si self-interstitials in the same way as for B and P. However, in the early stage of annealing (820°C, 1 min), a suppression of transient As diffusion is observed in samples implanted with higher As and Si doses. This suppression is most likely to be caused by the formation of immobile As–V clusters, as evidenced by the disappearance of the initial suppression in the sample implanted with Si at 15 keV, in which excess vacancies are distributed close to the surface.

Acknowledgements

The authors would like to thank Scott Dunham of the University of Washington for valuable discussion and comments. This work was financially supported by the Semiconductor Technology Academic Research Center (STARC).

1) Y. Kim, H. Z. Massoud and R. B. Fair: J. Electron. Mater. **18** (1989) 143.
2) D. J. Eaglesham, P. A. Stolk, H.-J. Gossmann and J. M. Poate: Appl. Phys. Lett. **65** (1994) 2305.
3) N. E. B. Cowern, G. F. A. van de Walle, P. C. Zalm and D. W. E. Vandenhoudt: Appl. Phys. Lett. **65** (1994) 2981.
4) H. S. Chao, S. W. Crowder, P. B. Griffin and J. D. Plummer: J. Appl. Phys. **79** (1996) 2352.
5) P. A. Stolk, H.-J. Gossmann, D. J. Eaglesham, D. C. Jacobson, C. S. Rafferty, G. H. Gilmer, M. Jaraiz, J. M. Poate, H. S. Luftman and T. E. Haynes: J. Appl. Phys. **81** (1997) 6031.
6) F. F. Morehead, B. L. Crowder and R. S. Title: J. Appl. Phys. **43** (1972) 1112.
7) S. Tian, M. F. Morris, S. J. Morris, B. Obradovic, G. Wang, A. F. Tasch and C. M. Snell: IEEE Trans. Electron Devices **45** (1998) 1226.
8) M. Tamura, Y. Hiroyama, A. Nishida and M. Horiuchi: Appl. Phys. A **66**(1998) 373.
9) J. Xia, T. Saito, T. Aoki, Y. Kamakura and K. Taniguchi: Jpn. J. Appl. Phys. **37** (1998) L913.
10) J. Xia, T. Saito, R. Kim, T. Aoki, Y. Kamakura and K. Taniguchi: J. Appl. Phys. **85** (1999) 7597.
11) S. Solmi, F. Cembali, R. Fabbri, M. Servidori and R. Canteri: Appl. Phys. A **48** (1989) 255.
12) R. Kim, Y. Furuta, S. Hayashi, T. Hirose, T. Shano, H. Tsuji and K. Taniguchi: Appl. Phys. Lett. **78** (2001) 3818.
13) R. Brindos, P. Keys, K. S. Jones and M. E. Law: Appl. Phys. Lett. **75** (1999) 229.
14) A. Sultan, S. Banerjee, S. List and V. McNeil: J. Appl. Phys. **83** (1998) 8046.
15) S. Aronowitz, H. Puchner and J. Kimball: J. Appl. Phys. **85** (1999) 3494.
16) D. J. Eaglesham, P. A. Stolk, H.-J. Gossmann, T. E. Haynes and J. M. Poate: Nucl. Instrum. Methods Phys. Res. B **106** (1995) 191.
17) J. Xia and K. Taniguchi: unpublished.
18) J. Xia, T. Saito, R. Kim, T. Aoki, Y. Kamakura and K. Taniguchi: Jpn. J. Appl. Phys. **38** (1999) 2319.
19) A. Maiti, T. Kaplan, M. Mostoller, M. F. Chisholm, S. J. Pennycook and S. T. Pantelides: Appl. Phys. Lett. **70** (1997) 336.
20) P. M. Rousseau, P. B. Griffin, W. T. Fang and J. D. Plummer: J. Appl. Phys. **84** (1998) 3593.
21) K. C. Pandey, A. Erbil, G. S. Cargill III, R. F. Boehme and D. Vanderbilt: Phys. Rev. Lett. **61** (1988) 1282.
22) U. Myler, P. J. Simpson, D. W. Lawther and P. M. Rousseau: J. Vac. Sci. & Technol. B **15** (1997) 757.
23) A. M. Mazzone: Phys. Status Solidi A **95** (1986) 149.
24) D. J. Eaglesham, T. E. Haynes, H.-J. Gossmann, D. C. Jacobson, P. A. Stolk and J. M. Poate: Appl. Phys. Lett. **70** (1997) 3281.
25) V. C. Venezia, T. E. Haynes, A. Agarwal, L. Pelaz, H.-J. Gossmann, D. C. Jacobson and D. J. Eaglesham: Appl. Phys. Lett. **74** (1999) 1299.